

Effect of the Deposition Temperature on the Corrosion Stability of TiO₂ Films Prepared by Metal Organic Chemical Vapor Deposition

R. A. Antunes^{1,*}, M. C. L. de Oliveira², M. F. Pillis³

¹ Engineering, Modeling and Applied Social Sciences Center (CECS), Federal University of ABC (UFABC), 09210-170, Santo André-SP, Brazil

² Electrocell Ind. Com. Equip. Elet. LTDA, Technology, Entrepreneurship and Innovation Center (CIETEC), 05508-000 São Paulo-SP, Brazil

³ IPEN/CNEN-SP, Av. Prof. Lineu Prestes 2242, 05508-000, São Paulo, SP, Brazil

Received: 7 November 2012 / *Accepted:* 10 December 2012 / *Published:* 1 January 2013

The aim of this study was to investigate the influence of the deposition temperature on the corrosion stability of the TiO₂ layers. A metal organic chemical vapor deposition (MOCVD) system was used to grow TiO₂ films at three different temperatures: 300°C, 400°C and 500°C. The electrochemical behavior of the films was assessed through electrochemical impedance spectroscopy (EIS) measurements, potentiodynamic polarization curves and chronoamperometric curves. The tests were performed in a sodium chloride solution at room temperature. The porosity of the different films was also determined using an electrochemical method. The morphologies of the coatings were characterized by field emission scanning electron microscopy (FE-SEM) through surface and cross-sectional images and X-ray diffraction (XRD). The results pointed to a marked effect of the deposition temperature on the structure of the TiO₂ layers. The structure of the films was closely related to their corrosion stability. The film formed at 400°C yielded the highest corrosion resistance.

Keywords: TiO₂ films; MOCVD; deposition temperature; corrosion

1. INTRODUCTION

Titanium dioxide (TiO₂) has received much attention due to its high refractory index and dielectric constant that make it attractive to optical and electrical applications [1,2]. Recently, it has been considered as a photocatalytic and antimicrobial material in the degradation of organic contaminants [3]. TiO₂ thin films combine biocompatibility, corrosion resistance, high hardness and low tendency to wear. As a consequence, several investigators have produced TiO₂ layers for

protective coatings of biomedical metallic alloys [4-6]. The potential of this material to improve the corrosion properties of a variety of metallic substrates has been explored in the literature. Li et al. [7] studied the corrosion behavior of a TiO₂-coated Mg-Ca biodegradable alloy in a simulated body fluid. The film was obtained using a sol-gel method. The corrosion current density obtained from potentiodynamic polarization curves was found to be almost three orders of magnitude lower for the TiO₂-coated material in comparison with the bare Mg-Ca alloy. Another example of the effectiveness of TiO₂ films at enhancing the anticorrosion properties of a metallic substrate was given by Bamoulid et al. [8]. They combined the use of a conversion coating and a sol-gel TiO₂ top-coat to protect a ferritic stainless steel against corrosion. The conversion layer was obtained by chemical oxidation of the stainless steel substrate in an acidic solution with specific additives. A salt spray test was carried out to assess the corrosion resistance of the coated specimens. The TiO₂-coated specimens withstood the salt spray test during 500 h while the bare specimens and the specimens coated with a single conversion coating presented clear signs of corrosion. Liu et al. [9] demonstrated the high stability of a nano-TiO₂ layer produced by vacuum dip-coating sol-gel method against corrosion of anodized high purity aluminum specimens. Electrochemical tests were performed in sterile seawater at room temperature. The results revealed that the corrosion current densities of the coated specimens were lower than those of the bare alloy.

The high anticorrosion performance of these films can be accomplished through several deposition routes. CVD methods have been profitably employed to deposit TiO₂ coatings on titanium and 316L [10,11]. Gluszek et al. [12] used plasma assisted chemical vapor deposition (PACVD) to grow TiO₂ coatings on the surface of surgical grade 316L specimens. The corrosion resistance of the coated specimens was assessed through polarization curves and EIS measurements in Ringer's solution. The presence of the TiO₂ layer eliminated pitting corrosion, extending the passivity region of the 316L specimens up to 3 V. The bare alloy presented a breakdown potential at approximately 0.2 V. The corrosion potential was shifted to nobler values and the corrosion current density decreased two orders of magnitude. Popescu et al. [13] evaluated the biocompatibility and the corrosion behavior of metal-organic chemical vapor deposition (MOCVD) TiO₂ coatings on titanium. An interesting contribution given by the authors was related to the influence of the deposition parameters on the morphology of the TiO₂ films and the corresponding effects on the biocompatibility and the corrosion resistance of the coated specimens. In this respect, the total pressure, deposition temperature and deposition time had a marked influence on the coating morphology as observed through SEM micrographs. The thickness and roughness of the film varied with the deposition parameters. Independently of the conditions the corrosion resistance of the titanium specimens was improved by the TiO₂ coatings. The best condition was for a deposition temperature of 400 °C at atmospheric pressure during 60 minutes. This condition yielded a film with dendritic crystals and a thickness of 2 μm.

Despite the importance of the deposition parameters on the corrosion resistance imparted by MOCVD-formed TiO₂ layers, detailed investigations on this subject are lacking in the literature. In this regard, this work aims to give a further understanding on the influence of the deposition temperature on the corrosion resistance of TiO₂ films produced by MOCVD. The morphology and porosity of the films are strongly affected by this parameter. Hence, the electrochemical behavior of the TiO₂ coatings

was correlated with the structural characteristics obtained from each processing temperature used in the preparation of the specimens.

2. EXPERIMENTAL

2.1 Preparation of the TiO₂ films

The growth of the TiO₂ films was performed in home-made horizontal MOCVD equipment. This equipment is comprised of a reaction chamber that consists of a quartz tube heated by a cold-wall infra-red furnace, a hot chamber that contains the organometallic (OM) precursor, and a vacuum pump that maintains the reaction chamber in a pressure lower than the atmospheric. The OM vapor conduction lines were kept warmed. Titanium tetra isopropoxide (Ti(OCH(CH₃)₂)₄) warmed at 35°C was used as titanium and oxygen sources. Nitrogen was used as carrier gas and purge gas. The deposition time was 1 h. Three deposition temperatures were tested: 500 °C, 400 °C and 300 °C. The flux of N₂ was 0.5 L.min⁻¹ and the growth pressure was 50 mbar inside the reaction chamber. For convenience, the substrates consisted of Si (100) wafers. This allows the easy fracturing of the wafers, after deposition, in order to observe the microstructures of the films obtained at each deposition temperature by FE-SEM. The electrochemical properties of the films could be also promptly assessed. Other researchers have employed silicon substrates to investigate the corrosion stability of thin films [14,15]. Prior to deposition, the wafers were cleaned in a solution of 5% H₂SO₄ in deionized water for 5 min, rinsed in deionized water, dried in nitrogen and immediately put into the reaction chamber. These specimens were, then, employed for FE-SEM analyses, XRD and electrochemical measurements.

2.2 Microstructural Characterization

2.2.1 XRD analyses

The XRD measurements were carried out on a Philips X'Pert diffractometer using Cu K α radiation and grazing geometry with an incident angle of 5°. These measurements were performed in the range of 2 θ values from 10-80 with steps of 0.03°.

2.2.2 FE-SEM analyses

The samples were analyzed in a FEI Quanta 600 scanning electron microscope (SEM) coupled with chemical analysis by energy dispersive (EDS). Both surface and cross-sectional images are presented. Cross-sections were produced by the cleavage of the silicon-coated specimens.

2.3 Electrochemical measurements

2.3.1 Corrosion resistance

The corrosion resistance of the TiO₂ coated-specimens was evaluated in a NaCl 3.5 wt.% solution at room temperature. Three different techniques were employed to characterize the electrochemical behavior of the films: electrochemical impedance spectroscopy (EIS), potentiodynamic polarization curves and chronoamperometric curves. A conventional three-electrode cell was used in all the measurements, with a platinum wire as the counter electrode and a saturated calomel electrode (SCE) as the reference. All the potentials mentioned in the text are given related to this reference. Before the measurements, the specimens were immersed during 24 h in the electrolyte. The EIS data were collected at the open circuit potential (OCP) over a frequency range from 100 kHz to 10 mHz at 10 points per decade; a sine wave with ± 10 mV amplitude was applied. Potentiodynamic curves were performed from -0.5 V versus the OCP up to +1.0 V versus the OCP at a scan rate of 1.0 mV.s⁻¹. The data collected were analyzed using GPES software to determine the corrosion potential (E_{corr}) and corrosion current density (i_{corr}) of each specimen. Chronoamperometric curves were obtained at a fixed potential of 0.5 V during 1800 s. All the measurements were performed with an Autolab PGSTAT 100 potentiostat/galvanostat equipped with a FRA (Frequency Response Analyser) module.

2.3.2 Film porosity

Elsener et al. [16] proposed an electrochemical method to estimate the porosity of thin films based on the use of equation (1):

$$P = \left(\frac{R_{p,s}}{R_p} \right) \times 10^{-|\Delta E_{\text{corr}}|/b_a} \quad (1)$$

The porosity of the film is estimated from the change of the corrosion potential ($\Delta E_{\text{corr}} = E_{\text{corr,substrate}} - E_{\text{corr,substrate+coating}}$) caused by the presence of the coating layer and from individual measurements of the polarization resistance (R_p) of the bare and coated substrate. In equation (1) $R_{p,s}$ is the polarization resistance of the bare substrate, R_p is the polarization resistance of the coated substrate and b_a is the anodic Tafel slope of the bare substrate. $R_{p,s}$, b_a and $E_{\text{corr,substrate}}$ are determined from separate measurements of the bare substrate. Several authors employed this equation to estimate the porosity of thin ceramic films [17,18]. The electrochemical parameters were derived from the polarization curves obtained according to the procedure described in the previous section.

3. RESULTS AND DISCUSSION

3.1 Microstructural analyses

3.1.1 XRD analyses

Figure 1 shows X-ray diffraction patterns for the films grown at 300, 400 and 500 °C. The peaks were indexed according to the JCPDS card No. 21-1272 which corresponds to the pure anatase phase. No signs of brookite or rutile were found. The film grown at 300 °C presents less diffraction peaks than those obtained at higher temperatures, indicating that it is less crystalline.

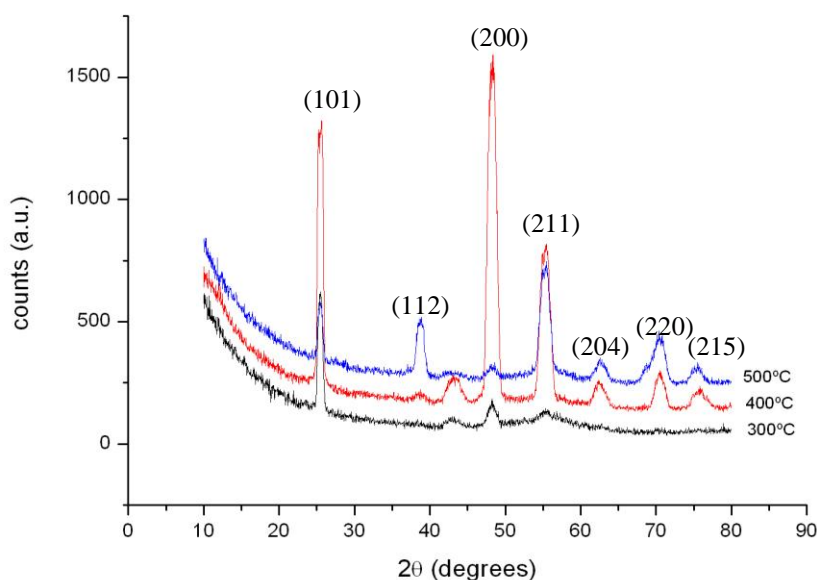


Figure 1. XRD grazing patterns (incident angle 5°) of the TiO₂ films.

3.1.2 SEM analyses

FE-SEM images of the TiO₂ films produced at different deposition temperatures are shown in Fig. 2. As indicated by the XRD analyses the films are comprised of the same crystalline phase. However, it is clearly seen that the morphology and thickness of the films were changed according to the deposition condition. The surface of the film formed at 300 °C presented a flat plate-like morphology as depicted in Fig. 2a. The coating was uniformly distributed throughout the whole surface. The cross-sectional view (Fig. 2b) revealed that the film was compact and very thin (approximately 32 nm). By increasing the temperature the films start to exhibit a columnar growth. The crystallites grow faster and the surface becomes rougher. This is shown in Fig. 2c and 2d for the film deposited at 400 °C. This phenomenon is more accentuated for the film deposited at 500 °C (Fig. 2e and 2f). The columnar structure is much more defined for the film obtained at 500 °C than at 400 °C. Hence, the temperature increment leads to a typical oriented crystal growth. Jung et al. [19] observed the same morphological features for TiO₂ films produced by a high-vacuum MOCVD

process. It is also noteworthy that the coating thickness is directly proportional to the deposition temperature in the range studied.

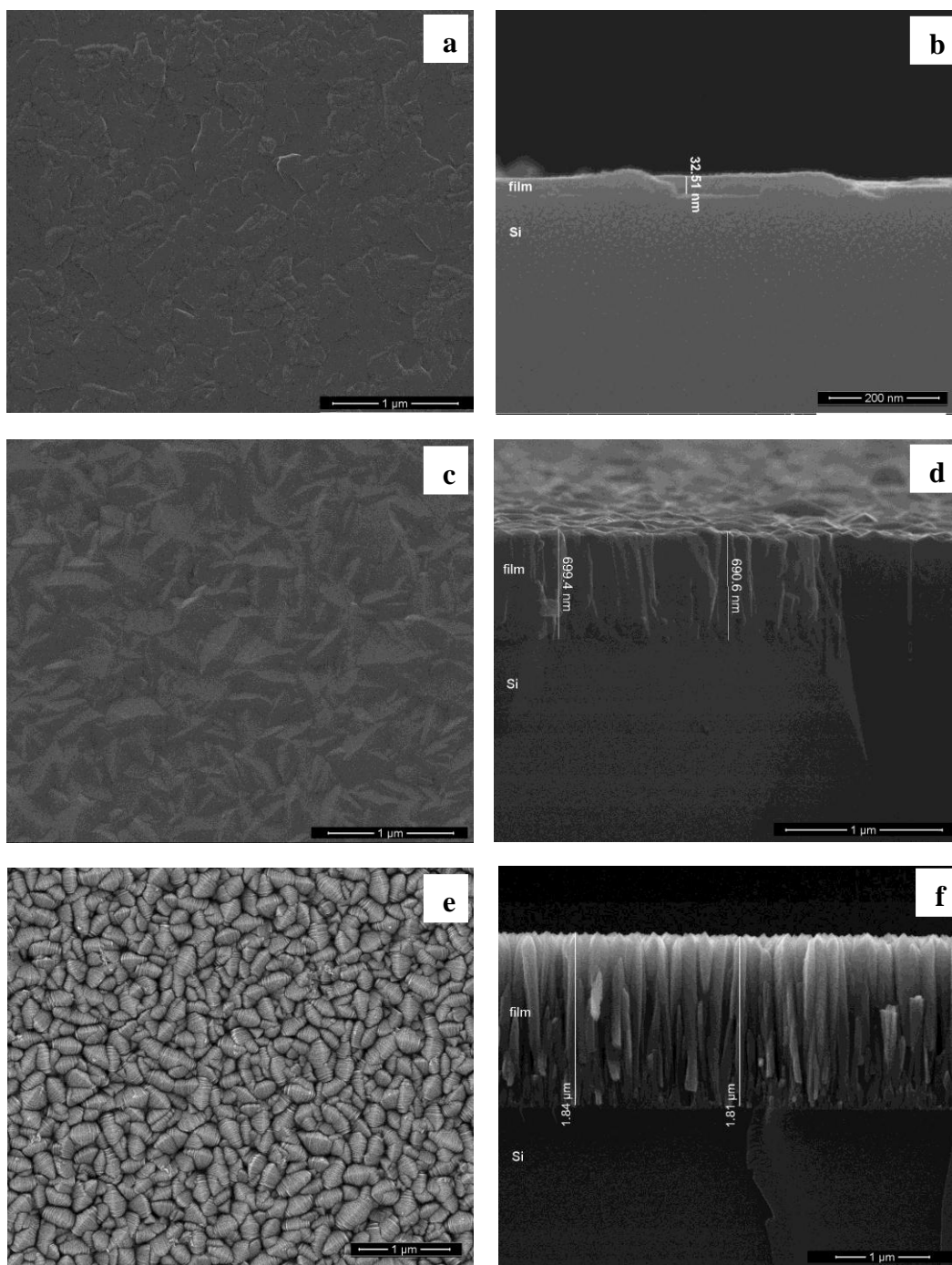


Figure 2. FE-SEM images of the TiO₂ films produced at different deposition temperatures: a) 300 °C, top view; b) 300 °C, cross-sectional view; c) 400 °C, top view; d) 400 °C, cross-sectional view; e) 500 °C, top view; f) 500 °C, cross-sectional view.

Duminica et al. [20] have also observed this growth mechanism for TiO₂ films produced by atmospheric pressure MOCVD. They observed that the coating thickness increased linearly with the

deposition time. Moreover, the films were more compact for lower deposition temperatures, whereas a well-defined columnar structure formed as the temperature was increased. Babelon et al. [21] have also studied the influence of the deposition temperature on the morphology of TiO₂ films grown by MOCVD on silicon substrates. It was found that the crystallite size increased with temperature similarly to the growth behavior observed in the present work. The same trend was depicted by Battiston et al. [22] for plasma enhanced-MOCVD-grown TiO₂ films. Mathur and Kuhn [23] evaluated the influence of the substrate temperature on the growth rate and morphology of TiO₂ coatings deposited by a low pressure-CVD process. Deposition was carried out in the temperature range 330-450 °C. The growth rate increased exponentially with increasing the substrate temperature, showing Arrhenius dependence and the control of the growth rate by surface reactions [24]. Above 450 °C the deposition rate began to drop. This behavior was due to a mass transport process. In this region, the diffusion of the precursor limits the film growth [20]. The microstructure of the TiO₂ films was also affected by the substrate temperature. Densely packed grains with faceted surfaces were obtained at 350 °C. A distinct morphology was achieved when the deposition temperature was 450 °C. The grains presented a columnar structure with clearly separated boundaries. The results obtained in the present work corroborate this trend as shown in Fig. 2. Jung et al. [25] confirmed that the microstructure of TiO₂ films deposited by low pressure-MOCVD at 500 °C presented columnar growth, forming prismatic crystals at the top surface that resembles those shown in Fig. 2e. The electrochemical behavior of thin films and their structure are markedly interconnected [26,27]. Next section deals with this subject, correlating the results obtained from EIS plots, potentiodynamic polarization and chronoamperometric curves with the structural features obtained at each of the deposition temperatures used in this work.

3.2 Corrosion Behavior

3.2.1 EIS measurements

Bode and Nyquist plots of the TiO₂-coated specimens are shown in Fig. 3. Independently of the deposition temperature, Bode plots presented a high frequency (HF) time constant characterized by a peak at approximately -57 °. This peak occurs at higher frequencies for the 400 °C-TiO₂ film, while it is shifted to lower frequencies for the films deposited at 300 °C and 500 °C. The peak shifting to lower frequencies is related to an increase in the HF time constant of the system. The time constant is the product of a capacitor and a resistor in parallel. Thus, this deviation can be caused by either capacitance or resistance changes. The area exposed to the electrolyte affects both parameters [28]. Moreover, the thickness of a thin film also affects the impedance of the associated constant phase element (CPE) [29]. The area in contact with the corrosive solution is a function of the porosity of the coating layer. This can lead to an unbalanced change of capacitance and resistance, thus shifting the time constant to lower frequencies. SEM images of the different CVD layers revealed that the 500 °C-TiO₂ film presented a well-defined columnar structure that favors the formation of open porosity through the coating [30]. Hence, as the porosity is expected to be higher in this layer, the HF time constant of the 500 °C-TiO₂ film occurs at the lowest frequency. The film deposited at 300 °C is the

most compact as seen in Fig. 2b. Thus, it is likely that the presence of through-coating porosity would be less intense on this film than on the films deposited at 400 °C and at 500 °C.

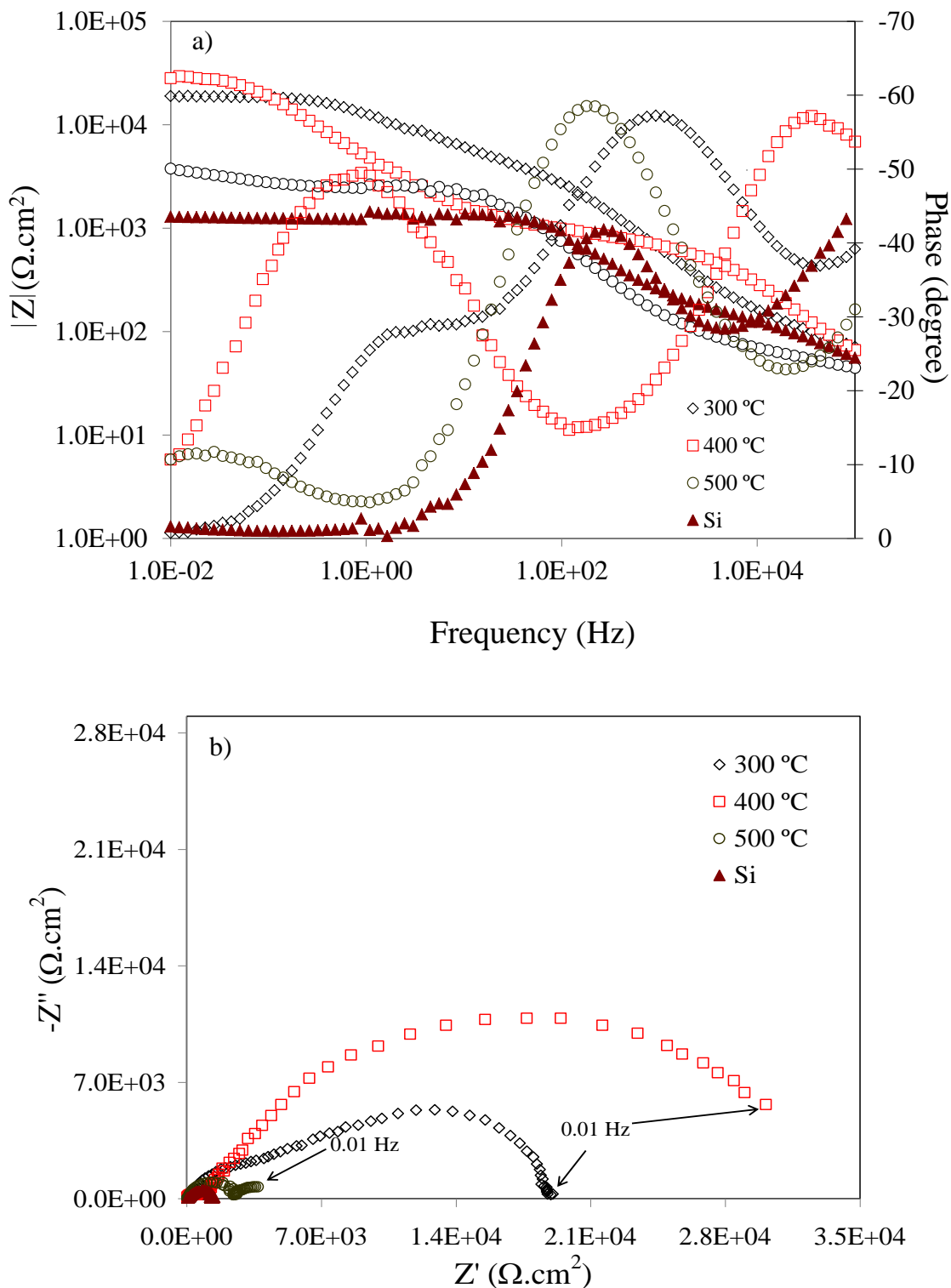


Figure 3. EIS data of the TiO₂-coated specimens obtained at different deposition temperatures and Si substrate: a) Bode and b) Nyquist plots.

However, as the 300 °C-deposited layer is also very thin in comparison with the other two conditions, it is also subjected to the same unbalanced change of capacitance and resistance that is likely to have occurred with the more defective 500 °C-deposited film. As a consequence, the HF time constant was also shifted to lower frequencies in comparison with the 400 °C-film. This film, in turn, has an intermediate morphology, i.e., it is less porous and thinner than the columnar 500 °C-film and less compact and thicker than the 300 °C-film. The HF time constant associated with the 400 °C-film is thereby at higher frequencies.

The time constant at lower frequencies is associated with the EIS response of the corrosion processes occurring at the interface between the TiO₂ films and the substrate. This time constant is characterized by a shoulder with a peak at approximately 1 Hz. In this regard, it is evident that the phase angles are more capacitive for the coating deposited at 400 °C. For the 300 °C-film this peak is less accentuated while it is barely defined for the 500 °C-film as seen in the Bode plots of Fig. 3a. High values of impedance modulus at low frequencies are associated with high corrosion resistance [31,32]. In this regard, it is noticeable that the impedance modulus of the 400 °C-film (28.2 kΩ.cm²) was higher than the values obtained for the 300 °C and 500 °C-films (18.9 and 3.7 kΩ.cm², respectively). The Si substrate, in turn, presented an impedance modulus of only 1.29 kΩ.cm².

Nyquist plots of Fig. 3b show that the films are characterized by a capacitive behavior independently of the deposition temperature. The impedance values evidence that the radius of the capacitive loop is higher for the 400 °C-film in comparison with the films deposited at 300 °C and 500 °C. This behavior suggests that the more corrosion-resistant material was achieved at 400 °C [33]. The 500 °C-film presented the lowest impedance values as shown in Fig. 3b. Hence, it is expected that the corrosion resistance of the films produced at 500 °C would be lower than for the films deposited at the other conditions. The differences observed in the Nyquist plots of the TiO₂ films probably arise from the distinct morphologies produced at each deposition temperature. The radius of the capacitive loop of the Si substrate was significantly smaller than that of the coated-specimens, revealing the increment of the corrosion resistance imparted by the MOCVD layers. This effect is less marked for the 500 °C-film.

3.2.2 DC Techniques

Potentiodynamic polarization curves of the TiO₂-coated specimens obtained at different deposition temperatures and of the Si substrate are shown in Fig. 4. The corresponding electrochemical parameters are presented in Table 1. The 500 °C-film presented the lowest value of corrosion potential (E_{corr}) and the highest value of corrosion current density (i_{corr}). The values were obtained by the Tafel's extrapolation method. The results point to the deficient corrosion resistance imparted by the coating obtained at 500 °C. In contrast, the film deposited at 400 °C presented the noblest E_{corr} and the lowest i_{corr} whereas the 300 °C-film presented intermediate values. The Si substrate presented the lowest corrosion resistance. Hence, the superior anticorrosion performance of the 400 °C-film is evidenced by the results shown in Table 1. This corroborates the analysis of the EIS data (section 3.2.1). In the same way, the intermediate performance of the 300 °C-film and the relatively poor anticorrosion properties

of the 500 °C-film are also consistent with the AC impedance results. Moreover, the anodic current densities are lower for the 400 °C-film throughout the whole potential range during anodic polarization in comparison with the other two coatings. Despite the noticeable differences between the electrochemical behaviors of the coatings deposited at each temperature, a common feature clearly distinguishable in the polarization curves shown in Fig. 5 has to be emphasized. Any of the polarization curves presented a steep increment of the current density as the potential increased. This behavior would be typical of the onset of film breakdown [34]. In this respect, the TiO₂ films were stable during the polarization tests, independently of the deposition temperature. This behavior is related to the typical high dielectric strength of TiO₂ that resists the collapsing of the film during polarization [35].

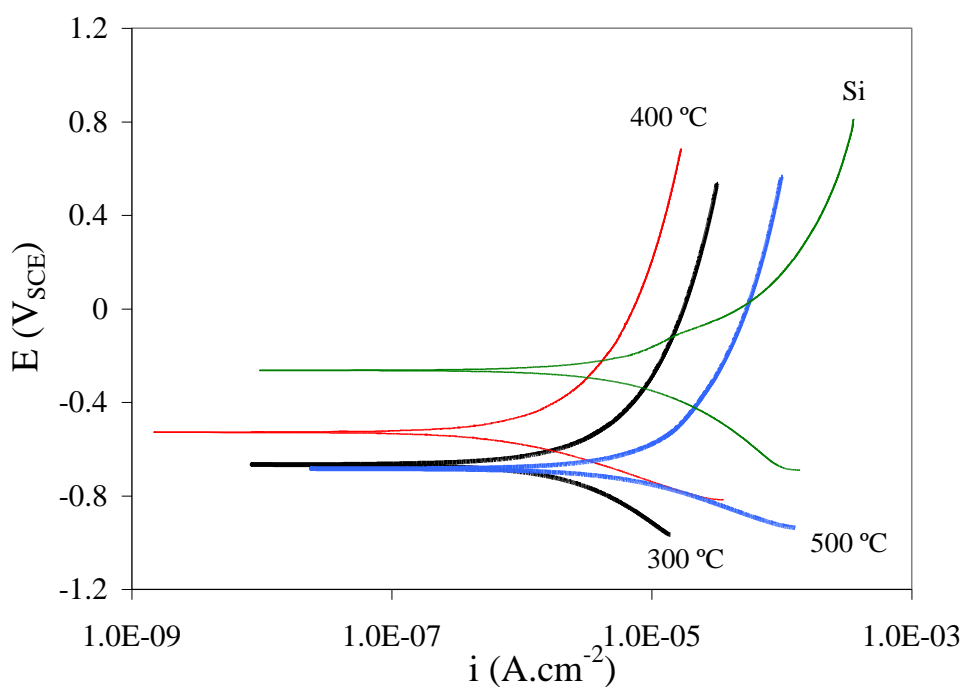


Figure 4. Potentiodynamic polarization curves of the TiO₂-coated specimens obtained at different deposition temperatures and Si substrate.

Table 1. Electrochemical parameters obtained from the potentiodynamic polarization curves shown in Fig. 4.

	300 °C	400 °C	500 °C	Si
E _{corr} (mV)	-667	-529	-685	-264
i _{corr} (μA.cm ⁻²)	0.06	0.04	0.20	1.42

In order to give a further insight into the electrochemical response of the TiO₂ films, chronoamperometric curves were obtained for the coated-specimens obtained at 300 °C, 400 °C and 500 °C. Bare Si is also shown for comparison. The results are shown in Fig. 5. The inset presents only the chronoamperometric curves of the coated-specimens to more clearly resolve the different current densities akin to each film. The current density dropped sharply in the very beginning of the test, indicating the passive nature of the TiO₂ films at the three conditions. The superior behavior of the 400 °C-film is confirmed as the current densities are lower for this condition throughout the whole test. The intermediate performance of the 300 °C-film is also evident. As expected, the current density of the Si substrate is significantly higher than those of the coated-specimens. The DC results are in line with the EIS data. The decisive influence of the coating structure was clearly observed. The deposition temperature employed during the MOCVD process is a key parameter regarding the anticorrosion properties of the resulting layers.

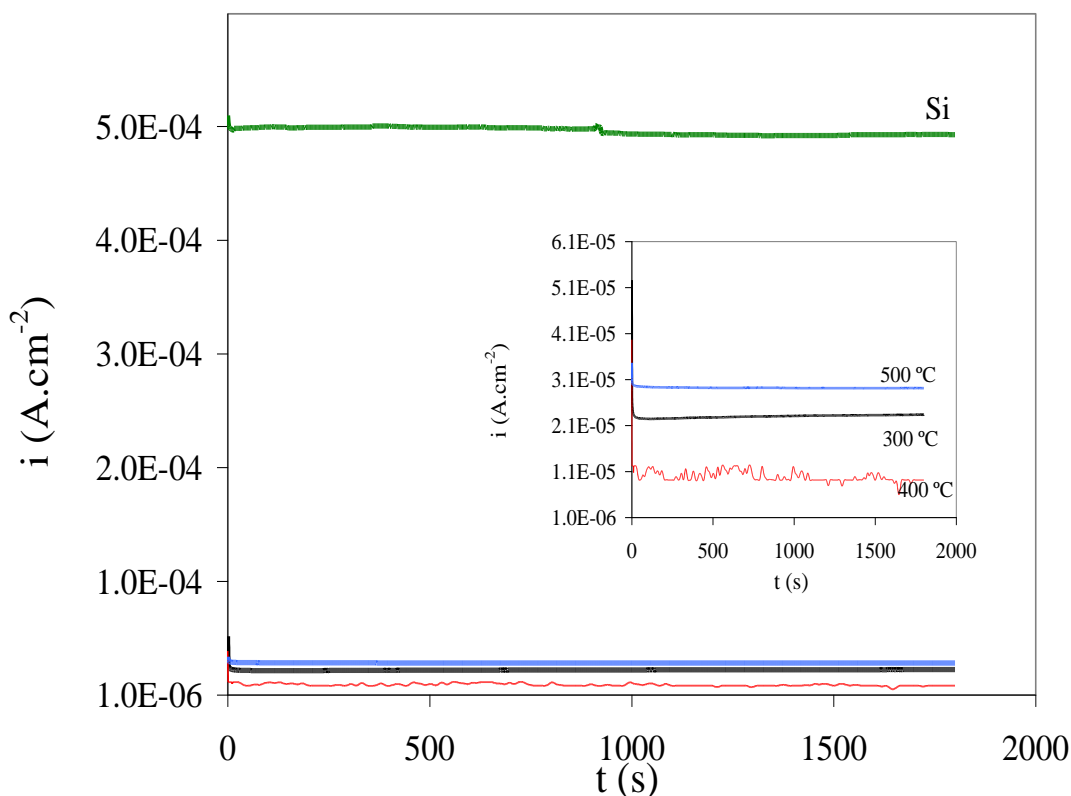


Figure 5. Chronoamperometric curves of the TiO₂ films obtained at different deposition temperatures and Si substrate.

3.2.3 Film Porosity

The results obtained from the polarization measurements of the bare and TiO₂-coated specimens are shown in Tab. 2. The film porosity was calculated according to equation (1). As seen in Fig. 2, the higher the deposition temperature, the less compact is the structure of the MOCVD film which shows a tendency of columnar growth. The results in Tab. 2 corroborate this visual indication.

The film produced at 300 °C presented the lowest porosity, followed by the film deposited at 400 °C whereas the 500 °C-film is the most porous. By comparing the porosity level with the corrosion resistance outcomes (sections 3.2.1 and 3.2.2) the following reasoning can be drawn: the film porosity plays a pivotal role for the corrosion protection ability of the TiO₂ films. The coating thickness seems to be of secondary importance since the thinnest film, that is, the 300 °C-film provided better corrosion resistance than the thickest film, i.e. the film produced at 500 °C. The film deposited at 400 °C has an intermediate porosity and thickness, achieving the best anticorrosion performance. We can hypothesize, though, that the corrosion stability of the coating obtained at 300 °C could be further improved if the deposition time was longer. It is worth remembering that the deposition time was set equal to all the MOCVD films (1 h as described in section 2.1). In this regard, if the compact structure achieved at 300 °C could be made thicker by extending the deposition time, the anticorrosion performance would be favorably affected. New experiments are in course to investigate this effect.

Table 2. Electrochemical parameters obtained from the polarization measurements and the corresponding porosity of TiO₂ films calculated according to equation (1).

Substrate			
$E_{\text{corr,substrate}}$ (mV)	$R_{p,s}$ ($\Omega \cdot \text{cm}^2$)	b_a (mV/decade)	
-264	10050	366	
TiO ₂ films			
Deposition temperature	$E_{\text{corr,substrate+coating}}$ (mV)	R_p ($\Omega \cdot \text{cm}^2$)	Porosity (%)
300 °C	-667	14420	5.52
400 °C	-529	11530	16.5
500 °C	-685	3923	18.1

4. CONCLUSIONS

TiO₂ films were prepared by MOCVD at different substrate temperatures. XRD analyses indicated that the films consisted of anatase phase independently of the deposition temperature. However, the deposition temperature has a marked influence on the morphology of the MOCVD TiO₂ films. SEM micrographs revealed that the film produced at 500 °C has a well-defined columnar structure and is thicker than the films obtained at lower temperatures. The most compact and thinnest layer was yielded at 300 °C. When the deposition temperature is increased to 400 °C the film grows at a faster rate, yielding a coating with intermediate thickness and relatively dense. These morphological issues proved to affect the corrosion resistance provided by the TiO₂ films. EIS measurements suggested that the columnar 500 °C-film was susceptible to electrolyte penetration. As a consequence, this deposition temperature provided the least corrosion-resistant layer. The potentiodynamic polarization curves and chronoamperometric curves confirmed this indication. The porosity level of

the films has been determined. The results confirmed that the 500 °C-coating was the most porous whereas the layer produced at 300 °C was the most compact. The film deposited at 400 °C yielded the best corrosion resistance due to its compactness and thickness. However, it is suggested that an increase of the thickness of the 300 °C through longer deposition times could improve its anticorrosion performance.

ACKNOWLEDGEMENTS

The authors are thankful to the Brazilian agency FAPESP (Proc. 05/55861-4) for the financial support to this work.

References

1. L. Escobar-Alarcón, E. Haro-Poniatowski, M.A. Camacho-López, M. Fernández-Guasti, J. Jiménez-Jarquín, A. Sánchez-Pineda, *Appl. Surf. Sci.* 137 (1999) 38.
2. Y.X. Leng, N. Huang, P. Yang, J.Y. Chen, H. Sun, J. Wang, G.J. Wan, X.B. Tian, R.K.Y. Fu, L.P. Wang, P.K. Chu, *Surf. Coat. Technol.* 156 (2002) 295.
3. C.-J. Chung, P.-Y. Hsieh, C.-H. Hsiao, H.-I Lin, A. Leyland, A. Matthews, J.-L. He, *Surf. Coat. Technol.* 203 (2009) 1689.
4. H. Hu, X. Liu, C. Ding, *J. Alloys Comp.* 498 (2010) 172.
5. R. Narayanan, S.K. Seshadri, *Mater. Chem. Phys.* 106 (2007) 406.
6. X. Liu, X. Zhao, B. Li, C. Cão, Y. Dong, C. Ding, P.K. Chu, *Acta Biomater.* 4 (2008) 544.
7. M. Li, Q. Chen, W. Zhang, W. Hu, Y. Su, *J Mater Sci.* 46 (2011) 2365.
8. L. Bamoulid, M.-T. Maurette, D. De Caro, A. Guenbour, A.B. Bachir, L. Aries, S. El Hajjaji, F. Benôit-Marquié, F. Ansart, *Surf. Coat. Technol.* 202 (2008) 5020.
9. T. Liu, F. Zhang, C. Xue, L. Li, Y. Yin, *Surf. Coat. Technol.* 205 (2010) 2335.
10. M.P. Casaletto, G.M. Ingo, S. Kaciulis, G. Mattogno, L. Pandolfi, G. Scavia, *Appl. Surf. Sci.* 172 (2001) 167.
11. P. Furman, J. Gluszek, J. Masalski, *J. Mater. Sci. Let.* 16 (1997) 471.
12. J. Gluszek, J. Masalski, P. Furman, K. Nitsch, *Biomaterials* 18 (1997) 789.
13. S. Popescu, I. Demetrescu, C. Sarantopoulos, A.N. Gleizes, D. Iordachescu, *J. Mater. Sci: Mater Med.* 18 (2007) 2075.
14. N.W. Khun, E. Liu, *Mater. Sci. Eng. C* 31 (2011) 1539.
15. E. Liu, H.W. Kwek, *Thin Solid Films* 516 (2008) 5201.
16. B. Elsener, A. Rota, H. Böhni, *Mater. Sci. Forum* 44-45 (1989) 29.
17. C. Liu, Q. Bi, A. Leyland, A. Matthews, *Corr. Sci.* 45 (2003) 1257.
18. W. Zhang, B. Tian, K.-Q. Du, H.-X. Zhang, F.-H. Wang, *Int. J. Electrochem. Sci.* 6 (2011) 5228.
19. C.-K. Jung, B.-C. Kang, H.-Y. Chae, Y.-S. Kim, M.-K. Seo, S.-K. Kim, S.-B. Lee, J.-H. Boo, Y.-J. Moon, J.-Y. Lee, *J. Crystal Growth* 235 (2002) 450.
20. F.-D. Duminica, F. Maury, F. Senocq, *Surf. Coat. Technol.* 188-189 (2004) 255.
21. P. Babelon, A.S. Dequiedt, H. Mostéfa-Sba, S. Bourgeois, P. Sibillot, M. Sacilotti, *Thin Solid Films* 322 (1998) 63.
22. G.A. Battiston, R. Gerbasi, A. Gregori, M. Porchia, S. Cattarin, G.A. Rizzi, *Thin Solid Films* 371 (2000) 126.
23. S. Mathur, P. Kuhn, *Surf. Coat. Technol.* 201 (2006) 807.
24. G.A. Battiston, R. Gerbasi, M. Porchia, A. Gaspararotto, *Chem. Vap. Deposition* 5 (1999) 13.
25. S.-C. Jung, B.-H. Kim, S.-J. Kim, N. Imaishi, Y.-I. Cho, *Chem. Vap. Deposition* 11 (2005) 137.

26. R.A. Antunes, A.C.D. Rodas, N.B. Lima, O.Z. Higa, I. Costa, *Surf. Coat. Technol.* 205 (2010) 2074.
27. C. Liu, Q. Bi, A. Leyland, A. Matthews, *Corr. Sci.* 45 (2003) 1243.
28. A. Zeng, E. Liu, I.F. Annergren, S.N. Tan, S. Zhang, P. Hing, J. Gao, *Diamond Relat Mater.* 11 (2002) 160.
29. J.R. Macdonald, W.R. Keenan, *Impedance Spectroscopy: Emphasizing Solid Materials and Systems*, John Wiley & Sons, USA, 1987.
30. C. Sarantopoulos, E. Puzenat, C. Guillard, J.-M. Hermann, A.N. Gleizes, F. Maury, *Appl. Catal. B: Environ.* 91 (2009) 225.
31. M.K.P Kumar, T.V Venkatesha, M.K Pavithra, N.A Shetty, *Phys Scr.* 84 (2011) 035601 (10 pp).
32. E. Alkhateeb, R. Ali, S. Virtanen, N. Popovsk, *Surf. Coat. Technol.* 205 (2011) 3006.
33. C. Liu, Q. Bi, H. Ziegele, A. Leyland, A. Matthews, *J Vac Sci Technol.* 20 (2002) 772.
34. J. Bolton, X. Hu, *J. Mater. Sci. Mater. Med.* 13 (2002) 567.
35. N. Padhy, S. Kamal, R. Chandra, U.K. Mudali, B. Raj, *Surf. Coat. Technol.* 204 (2010) 2782.